



Title	Magnetic properties of epitaxial Fe ₃ O ₄ films with various crystal orientations and tunnel magnetoresistance effect at room temperature
Author(s)	Nagahama, Taro; Matsuda, Yuya; Tate, Kazuya; Kawai, Tomohiro; Takahashi, Nozomi; Hiratani, Shungo; Watanabe, Yusuke; Yanase, Takashi; Shimada, Toshihiro
Citation	Applied Physics Letters, 105(10), 102410 https://doi.org/10.1063/1.4894575
Issue Date	2014-09-08
Doc URL	http://hdl.handle.net/2115/57532
Rights	Copyright 2014 American Institute of Physics. This article may be downloaded for personal use only. Any other use requires prior permission of the author and the American Institute of Physics. The following article appeared in Applied Physics Letters 105, 102410 (2014); and may be found at http://dx.doi.org/10.1063/1.4894575
Type	article
File Information	1.4894575.pdf



[Instructions for use](#)

Magnetic properties of epitaxial Fe₃O₄ films with various crystal orientations and tunnel magnetoresistance effect at room temperature

Taro Nagahama, Yuya Matsuda, Kazuya Tate, Tomohiro Kawai, Nozomi Takahashi, Shungo Hiratani, Yusuke Watanabe, Takashi Yanase, and Toshihiro Shimada

Citation: *Applied Physics Letters* **105**, 102410 (2014); doi: 10.1063/1.4894575

View online: <http://dx.doi.org/10.1063/1.4894575>

View Table of Contents: <http://scitation.aip.org/content/aip/journal/apl/105/10?ver=pdfcov>

Published by the [AIP Publishing](#)

Articles you may be interested in

[Study of site-disorder in epitaxial magneto-electric GaFeO₃ thin films](#)

Appl. Phys. Lett. **102**, 212401 (2013); 10.1063/1.4807757

[Giant tunneling magnetoresistance up to 410% at room temperature in fully epitaxial Co/MgO/Co magnetic tunnel junctions with bcc Co\(001\) electrodes](#)

Appl. Phys. Lett. **89**, 042505 (2006); 10.1063/1.2236268

[Giant tunneling magnetoresistance in fully epitaxial body-centered-cubic Co/MgO/Fe magnetic tunnel junctions](#)

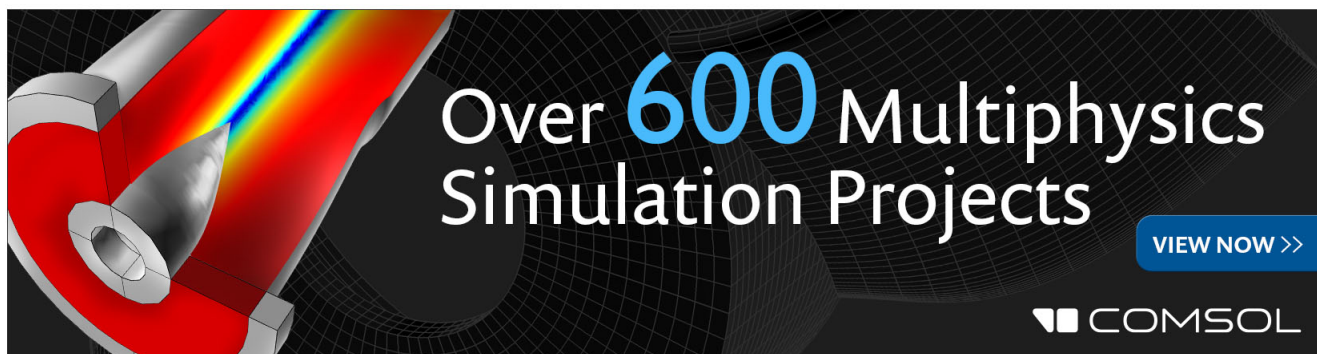
Appl. Phys. Lett. **87**, 222508 (2005); 10.1063/1.2138355

[Structural and magnetic properties of epitaxial L₂1-structured Co₂\(Cr, Fe\)Al films grown on GaAs\(001\) substrates](#)

J. Appl. Phys. **97**, 103714 (2005); 10.1063/1.1888050

[Nanoscale phase separation in Fe₃O₄ \(111\) films on sapphire\(0001\) and phase stability of Fe₃O₄ \(001\) films on MgO\(001\) grown by oxygen-plasma-assisted molecular beam epitaxy](#)

J. Appl. Phys. **93**, 5626 (2003); 10.1063/1.1556174

An advertisement for COMSOL Multiphysics. It features a 3D cutaway view of a mechanical part with a colorful stress or temperature distribution. The text 'Over 600 Multiphysics Simulation Projects' is prominently displayed in white and blue. A blue button with the text 'VIEW NOW >>' is located in the bottom right corner. The COMSOL logo is in the bottom right corner.

Magnetic properties of epitaxial Fe₃O₄ films with various crystal orientations and tunnel magnetoresistance effect at room temperature

Taro Nagahama,^{a)} Yuya Matsuda, Kazuya Tate, Tomohiro Kawai, Nozomi Takahashi, Shungo Hiratani, Yusuke Watanabe, Takashi Yanase, and Toshihiro Shimada
 Graduate School of Engineering, Hokkaido University, Kita13 Nishi8, Kitak-ku, Sapporo 060-8628, Japan

(Received 5 June 2014; accepted 22 August 2014; published online 12 September 2014)

Fe₃O₄ is a ferrimagnetic spinel ferrite that exhibits electric conductivity at room temperature (RT). Although the material has been predicted to be a half metal according to *ab-initio* calculations, magnetic tunnel junctions (MTJs) with Fe₃O₄ electrodes have demonstrated a small tunnel magnetoresistance (TMR) effect. Not even the sign of the tunnel magnetoresistance ratio has been experimentally established. Here, we report on the magnetic properties of epitaxial Fe₃O₄ films with various crystal orientations. The films exhibited apparent crystal orientation dependence on hysteresis curves. In particular, Fe₃O₄(110) films exhibited in-plane uniaxial magnetic anisotropy. With respect to the squareness of hysteresis, Fe₃O₄ (111) demonstrated the largest squareness. Furthermore, we fabricated MTJs with Fe₃O₄(110) electrodes and obtained a TMR effect of -12% at RT. The negative TMR ratio corresponded to the negative spin polarization of Fe₃O₄ predicted from band calculations. © 2014 AIP Publishing LLC. [<http://dx.doi.org/10.1063/1.4894575>]

Half metals that have 100% spin polarization (P) at the Fermi level are key materials to fabricate spintronic devices because their high spin polarization enables very large magnetoresistance effects. The most impressive case is in magnetic tunnel junctions (MTJs) with epitaxial MgO tunnel barriers.^{1,2} As transport in MgO-MTJs is dominated by coherent tunneling of Δ_1 electrons with 100% spin polarization, the tunnel magnetoresistance (TMR) ratio has reached 600% at room temperature (RT).³ Such a large TMR ratio has allowed us to fabricate highly functional spintronic devices like magnetoresistive random access memories (MRAMs). However, MTJs with MgO have stringent limitations where the crystal orientation should be bcc (001) due to band structure matching between MgO and the electrodes. Half metal is the solution to large TMR ratios without restricting the crystal structure or orientation. Thus, far, many oxide materials have been proposed as candidates for half metals, e.g., CrO₂,⁴ La_{0.7}Sr_{0.3}MnO₃,⁵ and Fe₃O₄.⁶ Of these materials, Fe₃O₄ has been considered to be the most promising as a half metal because of its high Curie temperature (T_c) of 858 K, which is an advantage in applications to spintronic devices that require high T_c . The crystal structure is an inverse spinel with Fe³⁺ cations occupying tetrahedral sites (A sites) and Fe³⁺ and Fe²⁺ cations occupying octahedral sites (B sites). The magnetic couplings between A and B sites are antiferromagnetic and the couplings at A-A or B-B are ferromagnetic; consequently, it is a ferrimagnetic material. As Fe₃O₄ exhibits good electric conductivity at RT due to the hopping of electrons between Fe²⁺ and Fe³⁺ on the B sites,⁷ the conduction electrons are 100% spin polarized. As hopping is frozen on cooling, conductivity greatly decreases at low temperature, which is known as Verwey transition. The transition temperature, T_v , is 120 K.⁸ The saturation magnetization of bulk Fe₃O₄ is 510 emu/cc.⁹ According to Julliere's formula,¹⁰ MTJs with Fe₃O₄ electrodes are

expected to exhibit very high TMR ratios due to large spin polarization. To date, researchers have fabricated MTJs with Fe₃O₄ and measured magnetoresistance; however, the TMR ratios have been small. Although the reason for this is not completely understood, such small TMR ratios can be attributed to imperfect antiparallel magnetic states in MTJs.¹¹ The magnetization process of Fe₃O₄ films should be improved to achieve clear parallel and antiparallel magnetic configurations. We prepared epitaxial Fe₃O₄ films with various crystal orientations, and investigated their crystalline qualities and magnetic properties. We also fabricated MTJs with Fe₃O₄ electrodes and observed a negative TMR effect of -12% .

The Fe₃O₄ thin films were prepared with three crystal orientations of (001), (110), and (111) by using a molecular beam epitaxy (MBE) system. The sample structures were:

- (1) an MgO(001) substrate/MgO (20 nm)/Fe₃O₄ (60 nm),
- (2) an MgO(110) substrate/MgO (20 nm)/Fe₃O₄ (60 nm), and
- (3) an Al₂O₃(0001) substrate/Pt (20 nm)/Fe₃O₄ (60 nm).

Following the deposition of MgO or Pt buffer layers, Fe₃O₄ thin film was formed by reactive deposition at a temperature (T_{sub}) of 300 °C in an O₂ atmosphere of 4×10^{-4} Pa. Then, the films were annealed at 600 °C for 30 min in an O₂ atmosphere. The partial pressure of O₂ gas was 1×10^{-4} Pa during annealing. All the samples were fabricated under the same growth conditions to enable the quality of Fe₃O₄ films to be compared. Epitaxial growth was observed with reflection high energy electron diffraction (RHEED) and the surface morphology was observed with atomic force microscopy (AFM). We also investigated the magnetization process at RT with a vibrating sample magnetometer (VSM).

Figs. 1(a) and 1(b) show the RHEED patterns of Fe₃O₄(100) before and after O₂ annealing at 600 °C for 30 min. The electron beam was incident along [100]. Fig. 1(c) is an AFM of Fe₃O₄(100) after annealing. A streak RHEED pattern can be observed in Fig. 1(a) meaning the

^{a)}nagahama@eng.hokudai.ac.jp

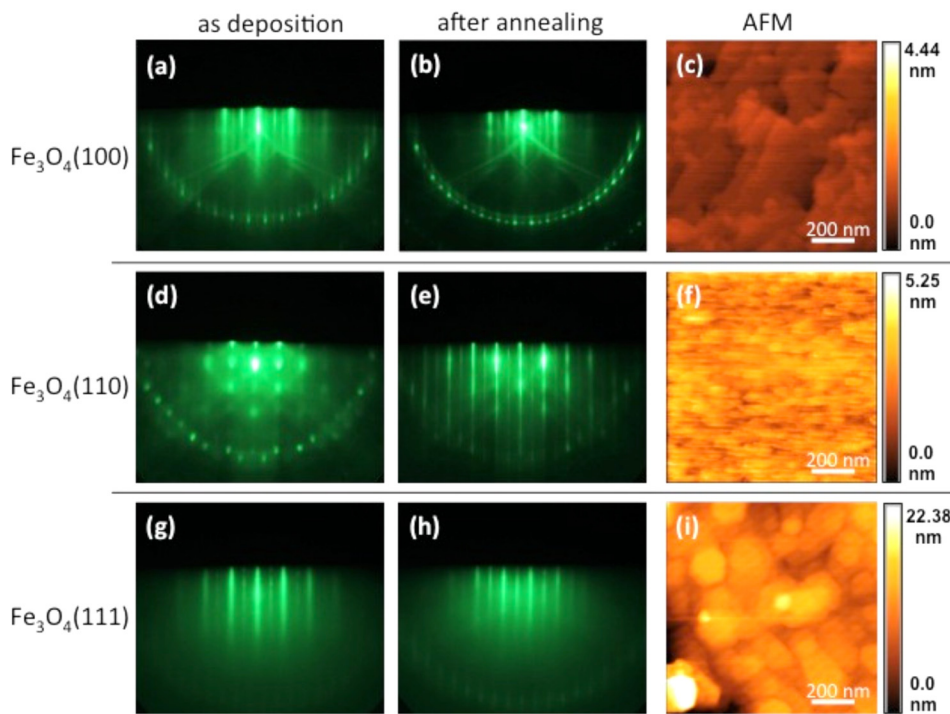


FIG. 1. RHEED patterns and AFMs of epitaxial Fe_3O_4 (60 nm) films. RHEED patterns were taken after deposition at 300°C and annealing at 600°C . AFM observations were carried out after annealing. (a), (b), and (c) are for $\text{MgO}(100)/\text{Fe}_3\text{O}_4(100)$ (60 nm). (d), (e), and (f) are for $\text{MgO}(110)/\text{Fe}_3\text{O}_4(110)$ (60 nm). (g), (h), and (i) are for $\text{Al}_2\text{O}_3(0001)/\text{Pt}(111)$ (20 nm)/ $\text{Fe}_3\text{O}_4(111)$ (60 nm).

Fe_3O_4 film grew epitaxially. In addition, $p(1 \times 1)$ surface reconstruction was observed.^{12,13} The streak pattern sharpened after annealing at 600°C in the O_2 atmosphere, as can be seen from Fig. 1(b). A step-terrace structure can be confirmed from the AFM in Fig. 1(c). The roughness average, R_a , was 0.12 nm, and the terrace width was 200 nm.

Figs. 1(d)–1(f) show the RHEED patterns and AFMs of $\text{Fe}_3\text{O}_4(110)$ grown on $\text{MgO}(110)$. The incident electron beam direction was $[-110]$. A spotty pattern was obtained before annealing due to the island growth of $\text{Fe}_3\text{O}_4(110)$. However, the surface flatness was improved dramatically by O_2 annealing at 600°C , as can be seen from the RHEED pattern in Fig. 1(e). The surface in the AFM of $\text{Fe}_3\text{O}_4(110)$ after annealing in Fig. 1(f) had anisotropic shapes along $[100]$, which seemed to originate from the anisotropy of the $\text{MgO}(110)$ substrate. R_a was estimated to be 0.39 nm.

Finally, Figs. 1(g)–1(i) show RHEED patterns and AFMs of $\text{Fe}_3\text{O}_4(111)$. The direction of the incident electron beam was $[11-20]$ Fig. 1(g) shows RHEED patterns of as-deposited $\text{Fe}_3\text{O}_4(111)$. It shows streak patterns that indicate a flat surface and surface reconstruction. Terrace and step structures can be observed in the AFM of $\text{Fe}_3\text{O}_4(111)$ after annealing in Fig. 1(i); however, islands with a diameter of 200 nm and height of several tens of nanometers were observed on the surface (not shown) in the AFM of a large area. The R_a was estimated at 2.40 nm, which was one order of magnitude larger than the other crystal orientations. The large roughness could be attributed to the lattice mismatch between Fe_3O_4 and the Pt buffer layer.¹⁴ As the lattice constant of Fe_3O_4 was 0.8397 nm and that of MgO was 0.421 nm, the lattice mismatch was about 0.3%. However, as the lattice constant of Pt was 0.392 nm, Fe_3O_4 lattice mismatch to the Pt buffer layer was 6.6%. Such large lattice mismatch could give rise to a larger surface roughness for $\text{Fe}_3\text{O}_4(111)$ than that for $\text{Fe}_3\text{O}_4(100)$.

The magnetization curves at RT for the Fe_3O_4 films are plotted in Fig. 2. The magnetic field was applied in plane. The diamagnetic components of the substrates were subtracted under the assumption that the magnetizations of the Fe_3O_4 were saturated at 5 kOe, which is the maximum field of VSM. The magnetization curve of $\text{Fe}_3\text{O}_4(100)$ is in Fig. 2(a). The saturation magnetization (M_s) was 330 emu/cc, the remanent magnetization (M_r) was 100 emu/cc, and the coercive field (H_c) was 80 Oe. The remanent magnetization ratio (M_r/M_s) was 0.30. Fig. 2(b) plots the magnetization curves of $\text{Fe}_3\text{O}_4(110)$ where the directions of the magnetic field were $[001]$ and $[-110]$. The saturation magnetization was 185 emu/cc for both magnetic field directions. M_r , H_c , and M_r/M_s in the magnetic field along $[001]$ were 30 emu/cc, 210 Oe, and 0.16, and those for $[-110]$ were 100 emu/cc, 780 Oe, and 0.54. The magnetization process strongly depended on the directions of the magnetic field, viz., the squareness and M_r/M_s were larger for the $[-110]$ magnetic field than those for $[100]$. Fig. 2(d) plots the dependence of the coercivity of $\text{Fe}_3\text{O}_4(110)$ film on the field angle measured with a MOKE system ($H_{max} = 2$ kOe). The H_c of the $\text{Fe}_3\text{O}_4(110)$ film indicated apparent uniaxial anisotropy. Nevertheless, the films had an anisotropic shape along the $[100]$ direction, as shown in Fig. 1(f), and the films had a larger remanent ratio in the $[-110]$ direction. Therefore, the anisotropy in Fig. 2(b) was attributed to the magnetocrystalline anisotropy in Fe_3O_4 . Saturation magnetization was 390 emu/cc, remanent magnetization was 290 emu/cc, and coercivity was 300 Oe in the magnetization curve of $\text{Fe}_3\text{O}_4(111)$. The remanent magnetization ratio was approximately 0.74, which was the largest value in the three crystal directions. The magnetic process was almost independent of the field directions. These values are summarized in Table I. All the films exhibited smaller saturated magnetizations than the value for bulk Fe_3O_4 of 510 emu/cc. The reason for this is that the external field was not sufficient to saturate the

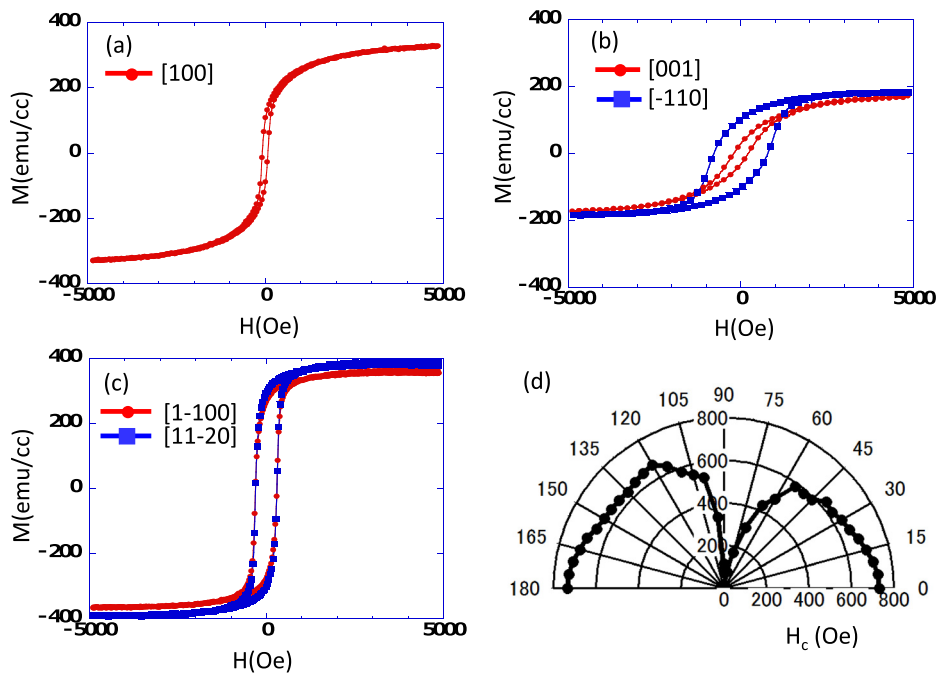


FIG. 2. Hysteresis curves obtained from VSM measurements at RT for epitaxial Fe_3O_4 films with various crystal orientations. (a) is $\text{Fe}_3\text{O}_4(100)$, (b) is $\text{Fe}_3\text{O}_4(110)$, and (c) is $\text{Fe}_3\text{O}_4(111)$. Directions of magnetic fields are given in plots. (d) is the coercive field, where the H_c of $\text{Fe}_3\text{O}_4(110)$ film is a function of the direction of the magnetic field. The angle is defined relative to the $[-110]$.

magnetic moments in the Fe_3O_4 films. According to previous studies, Fe_3O_4 thin films contain considerable numbers of antiphase boundaries (APBs)¹⁵ that make the Fe_3O_4 hard to saturate magnetically due to antiferromagnetic coupling at the APBs.

We fabricated the MTJs with $\text{Fe}_3\text{O}_4(110)$ electrodes, and measured the tunnel magnetoresistance effect. The film structure was $\text{MgO}(110)/\text{NiO}(110)$ (5 nm)/ $\text{Fe}_3\text{O}_4(110)$ (60 nm)/ Al_2O_3 (2.4 nm)/Fe (5 nm)/Co (10 nm)/Au (30 nm). The NiO layer was inserted to suppress the diffusion of Mg from the substrates. Junctions of $10 \times 10 \mu\text{m}^2$ were fabricated by photolithography, Ar ion milling, and sputtering. The junctions demonstrated a clear TMR effect of -12% at RT, as shown in Fig. 3(a). The negative MR agreed with the *ab-initio* calculations that predicted negative spin polarization in Fe_3O_4 . According to band calculations, the majority band of Fe_3O_4 has a bandgap at the Fermi level, so that conduction electrons have minority spin, meaning negative spin polarization.⁶ On the other hand, the Fe electrode with the Al_2O_3 barrier was experimentally found to have positive spin polarization.²¹ Therefore, a negative MR ratio was expected in $\text{Fe}_3\text{O}_4/\text{Al}_2\text{O}_3/\text{Fe}$ MTJs. To the best of our knowledge, these are the first experimental results of a negative MR ratio with an Al_2O_3 barrier and Fe_3O_4 electrodes.^{16–20} The polarization of Fe_3O_4 deduced from the MR ratio based on Julliere's formula was -16% , in which the polarization of Fe/ Al_2O_3 was assumed to be 40% .²¹ Although the polarization was much smaller than the predicted value, -16% is

of the same order as the reported values using various barrier materials.^{22,23}

With respect to the dependence on bias, the MR ratio had negative values in the range of ± 1 V, and the absolute value basically decreased with large bias voltage. The MR ratio remained at about -12% in the small bias region, which may be associated with the electric structure of Fe_3O_4 .

TABLE I. Magnetic characteristics of Fe_3O_4 films with various crystal orientations.

	M_s (emu/cc)	M_r (emu/cc)	H_c (Oe)	M_r/M_s
$\text{Fe}_3\text{O}_4(100)$	330	100	80	0.30
$\text{Fe}_3\text{O}_4(110)$ H//[001]	185	30	210	0.16
$\text{Fe}_3\text{O}_4(110)$ H//[-110]	185	100	780	0.54
$\text{Fe}_3\text{O}_4(111)$	390	290	300	0.74

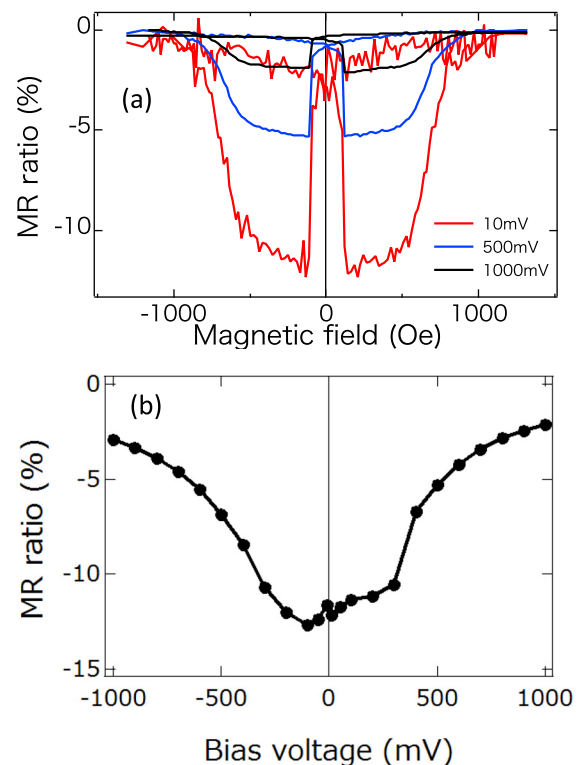


FIG. 3. (a) TMR curve for MTJ of $\text{MgO}(110)/\text{NiO}(110)$ (5 nm)/ $\text{Fe}_3\text{O}_4(110)$ (60 nm)/ Al_2O_3 (2.4 nm)/Fe (5 nm)/Co (10 nm)/Au (30 nm) at RT. Red, blue, and black lines are TMRs with bias voltages of 10, 500, and 1000 mV. (b) Dependence on bias of TMR ratio. Direction of bias voltage is defined with respect to upper electrode.

Theoretical investigations into transport properties are necessary to interpret the dependence on bias in detail.

Fe₃O₄ epitaxial films with various crystal orientations were fabricated by reactive MBE and all the films grew epitaxially. The Fe₃O₄ (110) films exhibited clear uniaxial magnetic anisotropy that originated from crystal anisotropy. The squareness of the hysteresis curves strongly depended on the crystal orientation. A negative MR ratio of −12% was observed in the MTJs with Fe₃O₄(110) electrodes. Although the absolute value was small, the negative MR agreed with the theoretical predictions.

We would like to express our gratitude to Professor Yamamoto's group for the cooperation in microfabrications. This work was supported by JSPS KAKENHI Grant-in-Aid for Young Scientists (A) Grant No. 23686006 and the Collaborative Research Program of Institute for Chemical Research, Kyoto University (Grant No. 2014-75).

- ¹S. Yuasa, T. Nagahama, A. Fukushima, Y. Suzuki, and K. Ando, "Giant room-temperature magnetoresistance in single-crystal Fe/MgO/Fe magnetic tunnel junctions," *Nat. Mater.* **3**, 868–871 (2004).
- ²S. S. Parkin, C. Kaiser, A. Panchula, P. M. Rice, B. Hughes, M. Samant, and S.-H. Yang, "Giant tunnelling magnetoresistance at room temperature with MgO (100) tunnel barriers," *Nat. Mater.* **3**, 862–867 (2004).
- ³S. Ikeda, J. Hayakawa, Y. Ashizawa, Y. Lee, K. Miura, H. Hasegawa, M. Tsunoda, F. Matsukura, and H. Ohno, "Tunnel magnetoresistance of 604% at 300 K by suppression of Ta diffusion in CoFeB/MgO/CoFeB pseudo-spin-valves annealed at high temperature," *Appl. Phys. Lett.* **93**, 082508 (2008).
- ⁴J. M. D. Coey and M. Venkatesan, "Half-metallic ferromagnetism: Example of CrO₂ (invited)," *J. Appl. Phys.* **91**, 8345–8350 (2002).
- ⁵B. Nadgorny, I. I. Mazin, M. Osofsky, R. J. Soulen, P. Broussard, R. M. Stroud, D. J. Singh, V. G. Harris, A. Arsenov, and Y. Mukovskii, "Origin of high transport spin polarization in La_{0.7}Sr_{0.3}MnO₃: Direct evidence for minority spin states," *Phys. Rev. B* **63**, 184433 (2001).
- ⁶A. Yanase and K. Siratori, "Band structure in the high temperature phase of Fe₃O₄," *J. Phys. Soc. Jpn.* **53**, 312–317 (1984).
- ⁷G. F. Dionne, *Magnetic Oxides* (Springer, 2010).
- ⁸E. Verwey, "Electronic conduction of magnetite (Fe₃O₄) and its transition point at low temperatures," *Nature* **144**, 327–328 (1939).
- ⁹S. Chikazumi, *Physics of Ferromagnetism 2e*, 94 (Oxford University Press, 2009).
- ¹⁰M. Julliere, "Tunneling between ferromagnetic films," *Phys. Lett. A* **54**, 225–226 (1975).
- ¹¹C. Tiusan, T. Dimopoulos, K. Ounadjela, and M. Hehn, "Field-dependent domain structure evolution in artificial ferrimagnets analyzed by spin-polarized tunnel transport in magnetic tunnel junctions," *Phys. Rev. B* **64**, 104423 (2001).
- ¹²S. A. Chambers, S. Thevuthasan, and S. A. Joyce, "Surface structure of Mbe-grown Fe₃O₄(001) by x-ray photoelectron diffraction and scanning tunneling microscopy," *Surf. Sci.* **450**, L273–L279 (2000).
- ¹³G. Tarrach, D. Bürgler, T. Schaub, R. Wiesendanger, and H.-J. Güntherodt, "Atomic surface structure of Fe₃O₄(001) in different preparation stages studied by scanning tunneling microscopy," *Surf. Sci.* **285**, 1–14 (1993).
- ¹⁴S. A. Chambers, "Epitaxial growth and properties of thin film oxides," *Surf. Sci. Rep.* **39**, 105–180 (2000).
- ¹⁵D. Margulies, F. Parker, M. Rudee, F. Spada, J. Chapman, P. Aitchison, and A. Berkowitz, "Origin of the anomalous magnetic behavior in single crystal Fe₃O₄ films," *Phys. Rev. Lett.* **79**, 5162 (1997).
- ¹⁶K.-I. Aoshima and S. X. Wang, "Fe₃O₄ and its magnetic tunneling junctions grown by ion beam deposition," *J. Appl. Phys.* **93**, 7945–7956 (2003).
- ¹⁷H. Matsuda, M. Takeuchi, H. Adachi, M. Hiramoto, N. Matsukawa, A. Odagawa, K. Setsune, and H. Sakakima, "Fabrication and magnetoresistance properties of spin-dependent tunnel junctions using an epitaxial Fe₃O₄ film," *Jpn. J. Appl. Phys., Part 2* **41**, L387–L390 (2002).
- ¹⁸M. Opel, S. Gepraegs, E. P. Menzel, A. Nielsen, D. Reisinger, K.-W. Nielsen, A. Brandlmaier, F. D. Czeschka, M. Althammer, M. Weiler *et al.*, "Novel multifunctional materials based on oxide thin films and artificial heteroepitaxial multilayers," *Phys. Status Solidi A* **208**, 232–251 (2011).
- ¹⁹P. Seneor, A. Fert, J.-L. Maurice, F. Montaigne, F. Petroff, and A. Vaurès, "Large magnetoresistance in tunnel junctions with an iron oxide electrode," *Appl. Phys. Lett.* **74**, 4017–4019 (1999).
- ²⁰C. Park, Y. Shi, Y. Peng, K. Barmak, J.-G. Zhu, D. Laughlin, and R. M. White, "Interfacial composition and microstructure of Fe₃O₄ magnetic tunnel junctions," *IEEE Trans. Magn.* **39**, 2806–2808 (2003).
- ²¹R. Meservey and P. Tedrow, "Spin-polarized electron tunneling," *Phys. Rep.* **238**, 173–243 (1994).
- ²²G. Hu and Y. Suzuki, "Negative spin polarization of Fe₃O₄ in magnetite/manganite-based junctions," *Phys. Rev. Lett.* **89**, 276601 (2002).
- ²³L. Alldredge, R. Chopdekar, B. Nelson-Cheeseman, and Y. Suzuki, "Spin-polarized conduction in oxide magnetic tunnel junctions with magnetic and nonmagnetic insulating barrier layers," *Appl. Phys. Lett.* **89**, 182504 (2006).